

DELIVERABLE REPORT



**D4.2: Full assessment
of degradation
mechanisms in NEXUS
high performing
PVSK/Si modules (> 12
months) (EURAC)**

**PREPARED BY EURAC
RESEARCH
COORDINATED BY
CEA**

NEXUS is a 3-year research and innovation project funded by the European Commission through the Horizon Europe Research and Innovation Action (RIA) grant N°101075330, responding to the call for a “Sustainable, secure and competitive energy supply” (HORIZON-CL5-2021-D3-02).

NEXUS aims to accelerate Europe’s energy transition by developing perovskite-silicon tandem photovoltaic technology, via a new European paradigm: an eco-design approach, based on efficiency, cost, sustainability, circularity and social aspects and using abundant materials. NEXUS aims to develop stable, 2-terminal perovskite-silicon tandem solar cells and modules with high power conversion efficiencies, using sustainable, coherent and competitive European PV production, to create a viable economic pathway for the European commercialisation of this technology.

NEXUS is formed of a multi-disciplinary consortium: 13 partners from 10 countries; 6 industrial partners & 7 RTOs, covering the whole value chain of innovation from research centres to technology providers, end-users and market and policies.

Project info	101075330 – NEXUS – HORIZON-CL5-2021-D3-02-04
Deliverable Title	D4.2- Full assessment of degradation mechanisms in NEXUS high performing PVSK/Si modules (> 12 months)
Lead Beneficiary	Eurac Research
Authors	J. Veirman, A. Louwen
Approved by	
Dissemination level	Sensitive/Public
Due date	October 2025
Submission date	
Version	V1
Linked to WP - task	WP4 – T4.3 Performance and reliability assessment of perovskite/Si tandem technology under real-life conditions

Legal notice

This document only reflects the authors' view, and the Union is not liable for any use that may be made of the information contained therein.

© This document is the property of the NEXUS Consortium. This document may not be copied, reproduced, or modified in whole or in part for any purpose without written permission from the NEXUS Consortium, which consists of the following participants:

NEXUS Consortium

Organization name	Short name	Country
COMMISSARIAT A L'ENERGIE ATOMIQUE ET AUX ENERGIES ALTERNATIVES	CEA	FR
ACCADEMIA EUROPEA DI BOLZANO	EURAC	IT
KARLSRUHER INSTITUT FUER TECHNOLOGIE	KIT	DE
RIJKSUNIVERSITEIT GRONINGEN	RUG	NL
SALD B.V	SALD	NL
UNIVERSITAT DE VALENCIA	UVEG	ES
3 SUN S.R.L.	3SUN	IT
ICARES CONSULTING	BI	BE
NORSUN AS	NORSUN	NO
THE CHANCELLOR, MASTERS AND SCHOLARS OF THE UNIVERSITY OF OXFORD	UOXF	UK
OXFORD PHOTOVOLTAICS LIMITED	OPV	UK
FACHHOCHSCHULE NORDWESTSCHWEIZ	FHNW	CH
ODTU GUNES ENERJISI UYGULAMA VE ARA STIRMA MERKEZI	GUNAM	TR



© Members of the NEXUS Consortium

Disclaimer

Funded by the European Union. Views and opinions expressed are however those of the author(s) only and do not necessarily reflect those of the European Union or CINEA. Neither the European Union nor the granting authority can be held responsible for them.

How to Cite

J. Veirman et al (2025). Deliverable D4.2 Report: Full assessment of degradation mechanisms in NEXUS high performing PVSK/Si modules (> 12 months). in Project NEXUS: Next Generation of Sustainable Perovskite-Silicon Tandem Cells (No. 101075330). European Union. SENSITIVE/PUBLIC [Communicate on DD/MM/YYYY].

Table of Content

Table of Content.....	4
List of Tables.....	4
List of Figures.....	5
Abbreviations and acronyms list	6
1. Executive Summary	6
1.1. Description of the deliverable content and purpose.....	6
1.2. Relation with other activities in the project	7
2. Monitoring setup details and overview of monitored PST devices	7
2.1. Testing Setups	7
2.2. Monitoring and Data Collection.....	7
2.3. Test Devices	8
3. Selection of devices and analysis of outdoor underperformance	9
3.1. Outdoor monitoring data and sample selection.....	9
3.2. Underperformance identification from outdoor data	10
3.2.1. Correlation between Irradiance and Performance Ratio	10
3.2.2. Intraday performance evolution and morning recovery	13
3.2.3. Energy loss: hard degradation vs. winter dip.....	15
3.3. Visual inspection of the two selected devices	16
4. Literature review and comparison with NEXUS results	17
4.1. Overview of outdoor stability results	17
4.2. Metastability in perovskite-containing devices	17
4.3. Influence of temperature on LSE effect.....	19
5. Discussion.....	20
6. Concluding remarks and outlook	22
References.....	23
Annex 1: Promising devices (<12 months monitoring)	24
Annex 2: Initial IV curves of the two studied PST devices.....	26

List of Tables

Table 1: Measurement parameters at the testing setup of Eurac Research in Bolzano, Italy.....	8
Table 2 – Test devices installed end of July 2024 at Eurac Research. Outdoor P_{STC} was estimated using first several days of monitoring with data points close to 1000W/m ² irradiances.....	8
Table 3 – Test devices installed Q1 2025 at Eurac Research. The initial P_{STC} could not be assessed outdoors as irradiances were too far off of 1000W/m ² at the period of installation.....	9
Table 4 Summary of year-on-year degradation rates experimentally measured during the outdoor monitoring campaign at Eurac Research, Bolzano, Italy.....	10

List of Figures

Figure 1: Test setup at Eurac Research, Bolzano, Italy. The PST devices are installed in black water collectors, to collect the runoff water for analysis at FHNW. 7

Figure 2 Samples with >1 year monitoring at Eurac Research, Bolzano, Italy. The PR values shown between brackets correspond to the full monitoring duration plotted on the graph (13 months). 10

Figure 3 Focus on the temperature-corrected performance ratio (PR) of the reference device and the two most stable devices monitored at Bolzano, Italy. 11

Figure 4 Daily temperature-corrected performance ratio (PR) of the reference device and the two best devices in this study, as a function of daily Global Plane-Of-Array (GPOA) irradiance. The color scale indicates the time since installation. The fits are log fits to the first 60 (blue) and last 60 (red) monitoring days of the monitoring period. The purple areas show the data points collected during the “winter dip”. 12

Figure 5 Performance Ratio (PR) evolution throughout high and low GPOA irradiance days at the beginning and at the end of the monitoring period, for both devices selected in this study. Maximum Power Point voltages and currents are normalized (see text). The inset photograph is illustrating the moment when the sun rises above the nearby mountain. 13

Figure 6 Yearly PR evolution and stages for B1_HT1 and corresponding Yield loss pareto. 15

Figure 7 Photographs of the two devices analyzed in this report (bottom B1_HP2, top B1_HT1). The devices are still up and running at the time of writing of this report. 16

Figure 8 Overview of existing literature on outdoor monitoring of PST devices as per September 2025. The best result of the present study is shown in the purple rectangle. 17

Figure 9 Typical materialization of the “Light-Soaking Effect” on single junction perovskite and PST devices during outdoor testing [4]. 18

Figure 10 Light-Soaking Effect kinetics for several consecutive days in March 2022, plotted as a function of the daily cumulative irradiation. The days featured “very similar irradiance conditions”. $V_{mpp,sim}$ is the expected V_{mpp} without LSE, as derived per simulations. Adapted from [4]. 19

Figure 11 Daily PR as a function of daily GPOA irradiance and a) average device temperature and b) maximum device temperature (this study). 20

Figure 12: a) Photograph of the O1 device from KIT and installed at GUNAM, Ankara, Türkiye. b) Efficiency tracking as a function of time (~3 months). Each data point was derived from a current-voltage measurement taken every 10 minutes. The sample is kept at maximum power point between two consecutive measurements. Monitoring start: August 2025. 24

Figure 13: a) Photograph of the sequentially evaporated (from UOXF) 4-cell tandem module from CEA and installed at GUNAM, Ankara, Türkiye. These cells incorporate the nanotextured Si with a thin ITO interlayer and the rear AZO electrode. b) Efficiency tracking as a function of time (~3 months). Each data point was derived from a current-voltage measurement taken every 10 minutes. The sample is kept at maximum power point between two consecutive measurements. Monitoring start: August 2025. 24

Figure 14: a) Photograph of the device from KIT (lamination at CEA) and installed at UVEG, Valencia, Spain. b) Efficiency tracking as a function of time (3 months). The sample is kept at maximum power point between two consecutive measurements. Monitoring start: February 2025. Monitoring start: July 2025. 25

Figure 15: a) Photograph of the device from Oxford Uni (lamination at CEA) and installed at Eurac Research, Bolzano, Italy. b) Temperature-corrected performance ratio as a function of time (roughly 7 months). The sample is kept at maximum power point throughout the monitoring campaign. Monitoring start: February 2025. 25

Figure 16: Initial current-voltage curves of the two studied PST devices, measured after lamination. 26

Abbreviations and acronyms list

Abbreviation	Meaning
DUT	Device Under Test
GPOA	Global Plane-of-Array
HJT	Silicon Heterojunction
LCOE	Levelized cost of electricity
LSE	Light-Soaking Effect
MPP	Maximum Power Point
PCE	Power conversion efficiency
PST	Perovskite-silicon tandem
PR	Performance Ratio
STC	Standard Test Conditions
V _{mpp} - I _{mpp}	Maximum Power Point voltage and current
WP	Work Package

1. Executive Summary

In this work, we analyse devices from the NEXUS project after more than 12 months of outdoor monitoring. The performance ratio evolution reveals a yearly background degradation of about 14% for the most stable devices, overlaid with a “winter dip” corresponding to performance losses under low-irradiance conditions (Section 3). Although a long way off the requirement for being commercially competitive with established Si PV, this 14% annual degradation sets a new benchmark for the PST community and results are analysed to derive recommendations for outdoor stability enhancements. Some examples of encouraging outdoor stability results are shown at the end of the report, on the latest devices installed outdoor at the different partners’ sites.

By examining the data at seasonal, daily, and hourly scales, we identify the main features of both effects and propose a (likely non-exhaustive) tentative degradation pathway leading to the observed device degradation (Section 5). Possible root causes of the “winter dip,” including a morning recovery effect dependent on irradiance and temperature, are discussed in Section 4. The front-runner devices are still under monitoring and have not yet been disconnected for indoor analysis to avoid altering their state; forensic investigations will follow to validate these hypotheses. Conclusions summarize key findings and recommendations for PST technology. Part of these results were presented at PVSEC 2025, Bilbao, Spain.

1.1. Description of the deliverable content and purpose

The purpose of the deliverable is to provide a detailed analysis of the behavior of the best devices in the project after >12 months of outdoor monitoring (reached early August 2025), with a particular focus on the origins of the observed underperformance. In this document, we start off with an overview of the field performance of all devices installed outdoor so far, and select the samples eligible for the analysis. We then recall the main properties of these top performing devices, before focusing on the key underperformances and salient features revealed by the outdoor data. Eventually, we summarize all observations and propose a theoretical framework that can qualitatively reproduce the observations made throughout the report.

1.2. Relation with other activities in the project

WP1- Perovskite top cell developments
WP2- Sustainable tandem cell integration
WP3- Tandem Modules Scalability and Equipment

2. Monitoring setup details and overview of monitored PST devices

2.1. Testing Setups

In the frame of Task 4.3, several outdoor monitoring setups have been implemented at NEXUS partners UVEG in Valencia, Spain, FHNW in Basel, Switzerland, EURAC Research in Bolzano, Italy, and GUNAM in Ankara, Türkiye.

In particular, the outdoor testing setup at Eurac Research in Bolzano, Italy was designed to assess the performance and reliability of encapsulated perovskite silicon tandem (PST) cells (see Figure 1). This setup has been operational and measuring NEXUS samples since July 26th, 2024. Due to delays in the reception of good-quality samples and/or technical issues, monitoring of relevant samples started at a later stage at the other test sites. As a consequence, >12 months monitoring data is currently available only from the test site of Eurac Research, Bolzano, the results of which will therefore be used to assess the degradation mechanisms of PST Nexus devices in this report.

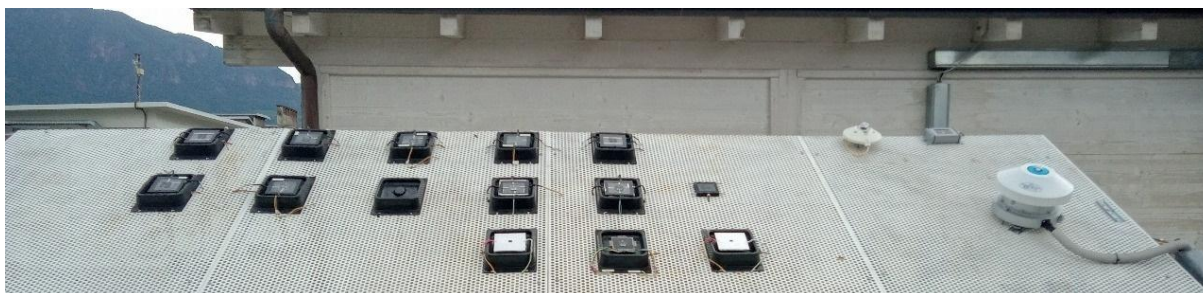


Figure 1: Test setup at Eurac Research, Bolzano, Italy. The PST devices are installed in black water collectors, to collect the runoff water for analysis at FHNW.

The test equipment for NEXUS' monitoring purposes installed at EURAC includes:

- A mounting frame with a steel sheet perforated with equally spaced round holes to enable flexible mounting and dismounting of NEXUS samples, installed at a tilt angle of 30 degrees from horizontal and an azimuth of 190 degrees from North.
- A micro-MPPT (μ MPPT) system for monitoring the electrical parameters of up to 22 devices under test (DUT) at maximum power point.
- A meteostation, pyranometer and reference cell sensors to measure solar irradiance and environmental conditions.
- Plastic moulded DUT holders developed by NEXUS partner FHNW, which capture any precipitation that falls on the DUTs and feeds it to collection cylinders.
- PT100 temperature sensors connected to the back of the DUTs in between the back glass and the sample holder DUT mounting point.

2.2. Monitoring and Data Collection

Monitoring of electrical performance began on July 27, 2024. The setup allows for continuous data acquisition to track:

- Performance stability of the samples.
- Possible Lead (Pb) emissions (material stability).
- Degradation of the samples over time.

The setup monitors a comprehensive set of measurement parameters including both the electrical measurements and temperature of the DUTs and the environmental conditions. The measurement parameters are listed below in Table 1.

Table 1: Measurement parameters at the testing setup of Eurac Research in Bolzano, Italy.

Parameter	Unit	Measured with	Notes
I_{mpp}	A	μMPPT	Current at maximum power
V_{mpp}	V		Voltage at maximum power
P_{mpp}	W		Maximum power point power
T_{DUT}	°C	Auxiliary monitoring	DUT backside temperature
GPOA irradiance	W/m ²		From pyranometer
GPOA irradiance	W/m ²		From reference cell
GPOA irradiance	W/m ²		From reference cell
Wind speed	km/h	Meteo Station	
Ambient air temperature	°C		
Precipitation intensity	mm/h		
Precipitation type	-		
Relative humidity	%		

2.3. Test Devices

Table 2 – Test devices installed end of July 2024 at Eurac Research. Outdoor P_{STC} was estimated using first several days of monitoring with data points close to 1000W/m² irradiances.



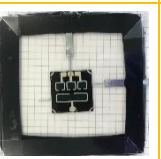





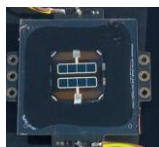
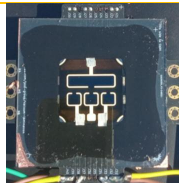
	RefHJT	EvapTex1 (ET1)	HybrTex1 (HT1)	HybrTex2a/b (HT2)	HybrPol1 (HP1)	HybrPol2a/b (HP2)
Sample description	2 minimodules, each made with 2 series-connected 1.5 x 3 cm ² silicon heterojunction (HJT) cells	1x 1 cm ² PST cell	1x 0.25 cm ² PST cell	1x 0.25 cm ² PST cell + 1x 1 cm ² PST cell, independently connected	1x 0.25 cm ² PST cell	1x 0.25 cm ² PST cell + 1x 1 cm ² PST cell, independently connected
Perovskite Deposition Process	n.a.	Evaporation	Hybrid	Hybrid	Hybrid	Hybrid
Wafer Type	Textured	Textured	Textured	Textured	Polished	Polished
Start Date	27-07-2024	27-07-2024	27-07-2024	27-07-2024	27-07-2024	27-07-2024
$P_{STC indoor}$	156.9 mW 162.6 mW	7.79 mW	3.69 mW	1.92 mW (0.25 cm ²) 9.19 mW (1 cm ²)	3.04 mW	4.10 mW (0.25 cm ²) 13.6 mW (1 cm ²)
$P_{STC outdoor}$	154.0 mW 157.9 mW	12.3 mW	8.21 mW	9.48 mW (0.25 cm ²) 23.0 mW (1 cm ²)	7.22 mW	9.81 mW (0.25 cm ²) 30.8 mW (1 cm ²)
Image						

Table 3 – Test devices installed Q1 2025 at Eurac Research. The initial P_{STC} could not be assessed outdoors as irradiances were too far off of $1000W/m^2$ at the period of installation.

	EvapText2 (ET2)	EvapPol1 (EP1)	EvapNanoText1 (EnT1)	EvapText3 (ET3)
Sample description	1x 0.25 cm ² PST cell + 1x 1 cm ² PST cell, independently connected	1x 0.25 cm ² PST cell + 1x 1 cm ² PST cell, independently connected	2 x 1.18 cm ² PST cells independently connected	Two PST cells, independently connected
Perovskite Deposition Process	Evaporation	Evaporation	Evaporation	Evaporation
Wafer Type	Textured	Chemically Polished	Nano-textured	Textured
Start Date	2025-02-19	2025-08-28	2025-03-03	2025-02-28
$P_{STC indoor}$	4.42 mW (0.25 cm ²) 17.03 mW (1 cm ²)	3.62 mW (0.25 cm ²) 18.26 mW (1 cm ²)	26.11 mW (1.18 cm ²) 27.16 mW (1.18 cm ²)	25.42 mW (1.18 cm ²) 27.60 mW (1.18 cm ²)
Image				

3. Selection of devices and analysis of outdoor underperformance

3.1. Outdoor monitoring data and sample selection

In this deliverable, and as explained above, we focus on those results with significant outdoor monitoring days so that >12 months of monitoring have been reached (as per the deliverable title). Given some technical issues and delays in the delivery/installation of samples outdoors, sufficient monitoring durations could only be reached at Eurac Research, and for that reason, **this report focuses hereafter solely on those results obtained at Eurac Research, Bolzano, Italy.**

Figure 2 shows the (outlier-filtered) temperature-corrected Performance Ratio (PR) for the 4 samples that feature >1 year monitoring with no hard failure throughout that period. PR is defined as $PR = \int P(t) dt / (P_{max} \times \int G_{POA_I}(t) dt)$, where $P(t)$ is the AC-side power, P_{max} is the STC measured device power and $G_{POA_I}(t)$ is the Global Plane Of Array Irradiance, and where the integrals are performed over a desired period of time. All samples are part of the first batch of samples delivered during summer 2024. They were all obtained using a hybrid process for the perovskite deposition (“H”) performed either on chemically polished (“P”) or textured (“T”) silicon heterojunction (HJT) bottom cells. It is worth noting that “P” and “T” types HJT bottom cells are both based on diamond-wire-sawn Cz Si wafers, which are standard in the PV industry, yet not very common among published results on PST devices. The daily PR values were calculated as the ratio between the measured energy output and the product of $P_{max}(T)$ and cumulative on-plane irradiance throughout the day. The temperature coefficient for P_{max} was taken as $-0.3\%/^{\circ}C$.

The 4 samples exhibit significantly different behaviour yet with some constant features: all samples show a pronounced degradation of their ability to convert the solar energy into electrical energy in a period of time from roughly October to March, with a pronounced “**winter dip**” on which

we will come back in detail in this report. All samples additionally show a significantly degraded PR after one year of operation that we refer to as “background degradation” in the following.

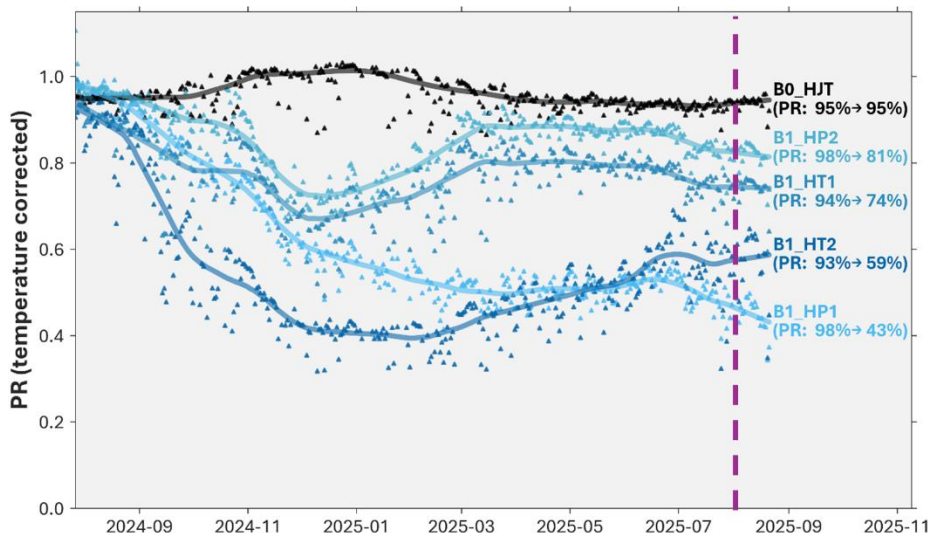


Figure 2 Samples with >1 year monitoring at Eurac Research, Bolzano, Italy. The PR values shown between brackets correspond to the full monitoring duration plotted on the graph (13 months).

Table 4 gathers the experimentally measured year-on-year degradation rates for the 4 samples in Figure 2 (from beginning of August 2024 to beginning of August 2025). While some of those samples suffered from very pronounced degradations, up to 50%, without obvious external root causes (suggesting inner cell degradation), B1-HP2 shows a more favourable behaviour with a year-on-year degradation of around 14. This value constitutes the most promising result in the scientific literature, as was advertised at the 42nd EU-PVSEC conference [1].

Table 4 Summary of year-on-year degradation rates experimentally measured during the outdoor monitoring campaign at Eurac Research, Bolzano, Italy.

#	Sample name	1 year PR degradation rate (%)
1	B1 – HP1	50.0
2	B1 – HT2	40.1
3	B1 – HT1	18.6
4	B1 – HP2	14.0

In this report, and in line with the aim of the deliverable, we focus on the two best performing samples, i.e. B1-HP2 and B1-HT1. Their performance is systematically compared to the reference HJT device, that serves as a benchmark throughout the report.

3.2. Underperformance identification from outdoor data

3.2.1. Correlation between Irradiance and Performance Ratio

The temperature-corrected daily PR data for the first 50 days is shown in Figure 3 for the two selected samples, together with the evolution of the daily Global Plane Of Array (GPOA irradiance) irradiance. Over that relatively short period, and given the results shown in Figure 2, a minor background degradation can be assumed for the samples. This timeframe can therefore be used to

check key features of fresh devices.

As can be observed, there is a clear correlation between PR and daily GPOA irradiance. All cells (including the reference HJT) exhibit a drop in PR on low GPOA irradiance days, and the drop amplitude is increasing with decreasing GPOA irradiance. **More importantly, this drop is markedly more pronounced for the PST devices than for the reference HJT.** For instance, on September the 12th, the drop is about 30% and 50% for PST devices while it is only about 15% for the HJT reference. Comparing the two PST devices, it is observed that the amplitude of the PR drop is higher for B1-HT1, which has the highest year-on-year degradation. It will be interesting in the future to investigate (more samples needed) whether more stable devices (i.e. with lower year-on-year degradation) are also less sensitive to low GPOA irradiance days.

Fortunately, the **PR drops are highly reversible**, meaning that on a high GPOA irradiance day the devices recover their saturated PR potential. For instance, the PR of B1_HP2 dropped from 0.87 on September the 3rd (high irradiance) down to 0.6 on September the 5th (particularly low irradiance) and then subsequently recovers back to 0.87 on September the 7th (high irradiance, similar as on September the 3rd). This recovery however is not that clear after the low GPOA irradiance event that happened on September the 12th (extremely low irradiance). Indeed, on the day before (11th September), the PR is at about 0.85, drops to 0.45 on September the 12th, and although September the 13th has a comparable GPOA irradiance as September the 11th, the PR does only partly recover to 0.67 (and not to the initial level, i.e. 0.85). Only after some average GPOA irradiance days does the PR recovers to 0.83 on the September the 18th (similar irradiance as on the initial day). This observation suggests a rather slow recovery of the properties after a very low irradiance day.

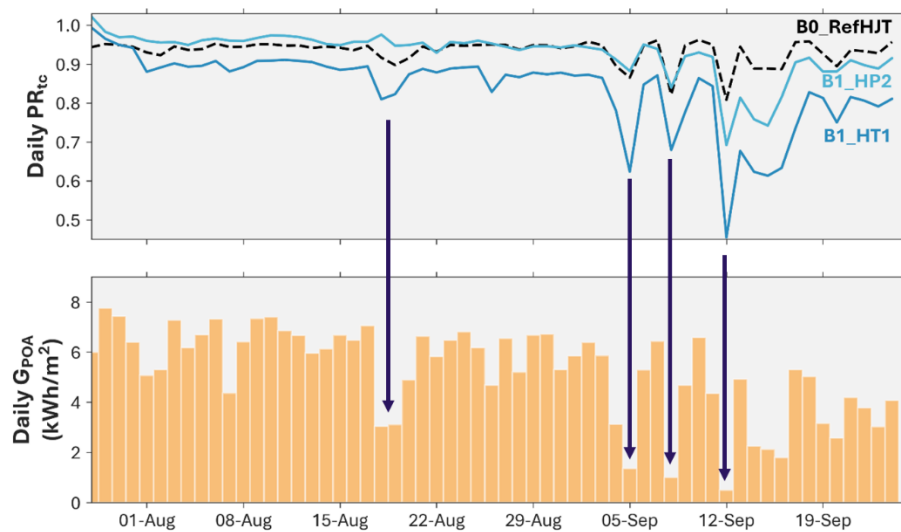


Figure 3 Focus on the temperature-corrected performance ratio (PR) of the reference device and the two most stable devices monitored at Bolzano, Italy.

In order to study how/if the PR underperformance on low GPOA irradiance days is evolving throughout the monitoring period, we plotted in Figure 4 the evolution (color scale) of the daily temperature-corrected PR as a function of daily GPOA irradiance. The blue and the red fits are log fits to the data from the first and the last 60-day periods, respectively (so August/September 2024 and 2025, respectively).

Regarding the reference HJT device, it can be observed that the PR remains little affected by the daily GPOA irradiance, as expected for the HJT technology [2]. Having a closer look at the HJT data during the first 60 days of operation (blue fit), the figure below reveals only about 10% PR variation between the highest and the lowest daily GPOA irradiance. In agreement with the very stable PR observed in Figure 2 for that technology, Figure 4 reveals a virtually unchanged dependence of the PR on GPOA irradiance throughout the monitoring period, highlighting the high stability of the device over the monitoring period.

Regarding the PST devices, Figure 4 calls for several comments:

- The poor behavior of the PST devices on days of low GPOA irradiance is confirmed throughout the monitoring period, with **daily PR plummeting on such dark days**.
- Focusing on the first 60 days of operation (fit in blue), the strongly decreasing PR with GPOA irradiance suggested in Figure 3 is clearly observed for both B1_HT1 and B1_HP2 (B1_HT1 being – again - more affected).
- The “winter dip” first reported in Figure 2 is also clearly observed (circled in purple). The PR values calculated in this region falls significantly below the PR of days with similar GPOA irradiances throughout the monitoring period, suggesting an **additional impact of low temperatures and/or of the red-shift of the spectrum**, typical of winter days in Bolzano, Italy.
- Although the data set remains limited, the initial and the final fits appear to cross at very low GPOA irradiance. This suggests that over the monitoring period, the behavior of both PST devices **does not degrade significantly (if at all) on such dark days**.
- Interestingly, the **amplitude of the drop between high and low GPOA irradiance days shrinks between the first and the last 60-day periods**. During the first 60-day period, the drop is indeed of about 30-40% of the PR at high GPOA irradiance days, whereas it is reduced to 20-30% in the last 60-day period (blue and red arrows, respectively).

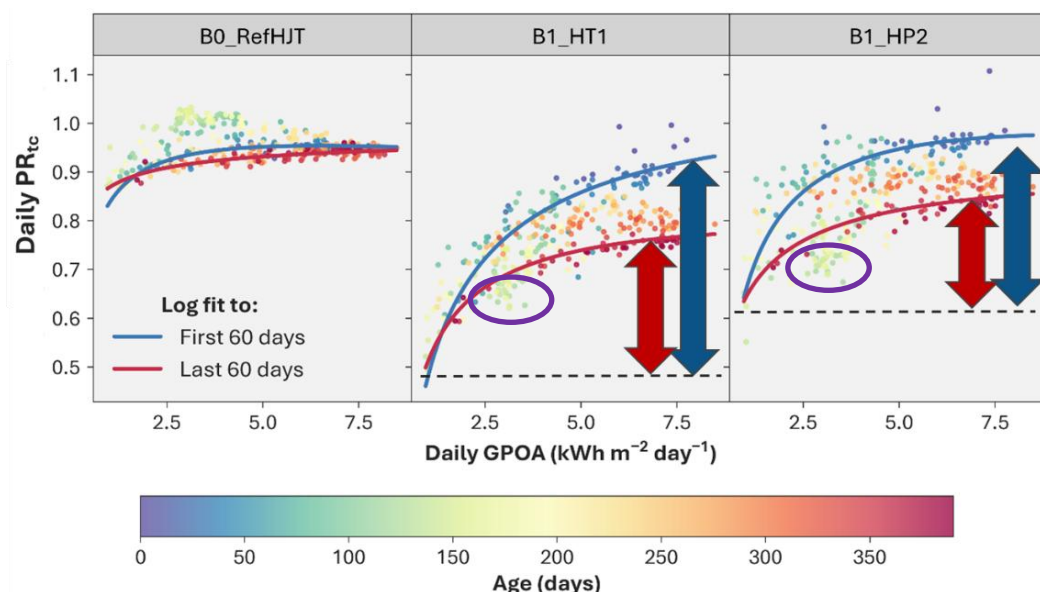


Figure 4 Daily temperature-corrected performance ratio (PR) of the reference device and the two best devices in this study, as a function of daily Global Plane-Of-Array (GPOA) irradiance. The color scale indicates the time since installation. The fits are log fits to the first 60 (blue) and last 60 (red) monitoring days of the monitoring period. The purple areas show the data points collected during the “winter dip”.

- ***Take-away messages: the devices exhibit a poor PR behavior on low GPOA irradiance days, but the low GPOA irradiance PR is virtually not degraded after 1 year. Conversely, the devices exhibit on average a comparatively high PR on days with high GPOA irradiance, but this behavior suffers strong degradation over time. One possible failure mode scenario could be an increase of the series resistance (explaining the drop in high GPOA irradiance days) while the shunt resistances (top and bottom cells) would remain largely unaffected (see Section 5 for more details). Last but not least, the PR in winter lies significantly below days of similar GPOA irradiances in the course of the year, suggesting an additional detrimental influence of temperature and/or the red-shift of the spectrum.***

3.2.2. Intraday performance evolution and morning recovery

In order to understand better the root cause(s) of the low performance at low GPOA irradiance, we plot in Figure 5 the evolution of the PR, normalized V_{mpp} and normalized I_{mpp} during a high and a low GPOA irradiance days (sunny and cloudy days, respectively), at the beginning and at the end of the monitoring period, and for the two samples of interest (B1_HT1 and B1_HP2). The initial and final days were chosen to have very similar GPOA irradiance and device temperature profiles during the course of the day. Normalization of V_{mpp} and I_{mpp} was performed to improve the graph readability. V_{mpp} and I_{mpp} were normalized throughout by their highest values around noon of the sunny infancy day. Finally, the orange inset shows the early hours of the day where the sun is behind a neighbouring mountain.

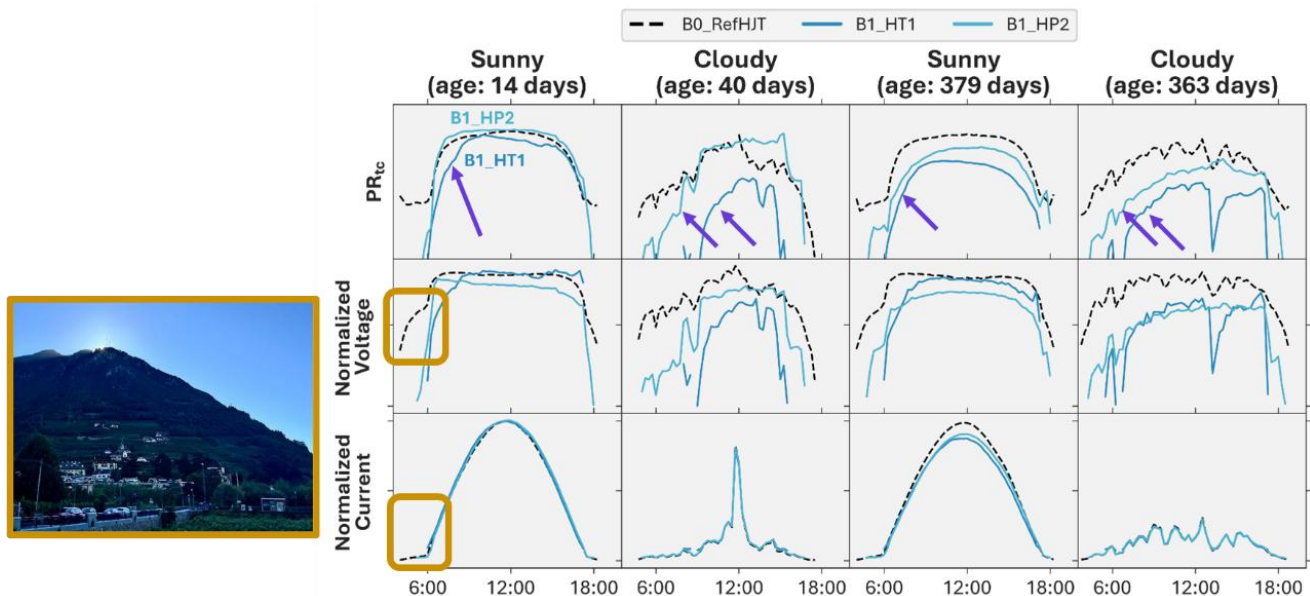


Figure 5 Performance Ratio (PR) evolution throughout high and low GPOA irradiance days at the beginning and at the end of the monitoring period, for both devices selected in this study. Maximum Power Point voltages and currents are normalized (see text). The inset photograph is illustrating the moment when the sun rises above the nearby mountain.

Several observations arise from Figure 5.

- On early-life sunny days:
 - o B1_HP2 is on-par with HJT once the sun is out (i.e. for most of the day).

- B1_HT1 shows a slow increase in PR during the first hours of direct sunlight, that is well correlated with the slow increase in V_{mpp} . The “recovery” is nevertheless fully effective after some hours only, i.e. until roughly 9am (purple arrow).
- *Take-away message: On high GPOA irradiance early days, samples either show similar behavior as the HJT (no lag) or need some time to reach their highpoint PR.*
- On early-life cloudy days:
 - Under cloudy conditions, B1_HP2 now also shows a lag/recovery period, also driven by the behavior of the V_{mpp} .
 - While B1_HT1 already needed some recovery time under sunny conditions, it now fails to recover, with PR values that remain very low, again driven by very low V_{mpp} .
 - *Take-away message: On low GPOA irradiance early days, both samples show an extended recovery period with no full recovery in the case of B1_HT1.*
- On late-life sunny days:
 - Although it did not have to recover on such sunny days in the early infancy, B1_HP2 now appears to need a recovery period on such days. Additionally, the peak PR is reduced, led by the overall device degradation already evidenced in Figure 2.
 - On the contrary, B1_HT1 shows a similar PR profile as during its infancy, except that - following the example of B1_HP2 - the peak PR is degraded.
 - *Take-away message: worsening of the recovery time superimposed by increased overall degradation.*
- On late-life cloudy days:
 - Both devices feature now very slow recoveries, only reaching their peak PR at around noon, while the HJT reference device already reached it at around 7-8am.
 - The max PR levels seem to be little affected since the early infancy period, in agreement with our analysis of Figure 4.
- Focus on the first hours of the day: until the sun rises above the neighboring mountain (5-6 am roughly in summer), the PR of all cells is low, but notably lower for the PST devices, which barely show any measurable output. This behavior could be accounted for by a combination of 1) slow morning recovery of the perovskite top cell and 2) the low relative amount of light received by the bottom cell when the sun is still hidden behind the mountain. Due to the mountain shadowing indeed, the spectrum does not contain any direct component, and is therefore exclusively diffusive (very blue-shifted). As a consequence, mostly the top cell is absorbing the available (low intensity) sunlight, while the bottom cell is only “seeing” a small fraction of it (depending on the EQE and the actual skylight spectrum), leading to a low voltage contribution from the bottom cell. The slow transients in the top cell efficiency evidenced above could also play a key role, perhaps even greater. When full spectrum sun-light is shone on a perovskite solar cell in a laboratory environment, the device generally takes seconds to minutes to reach a steady-state peak efficiency (See deliverable D3.3 for more information). Under these very low light level conditions of early morning, whilst the sun is shadowed by the mountain, the PST can be considered to be “un-activated” and it only “switches on” once the brightness or absorbed photon dose reaches a certain threshold. Shunts, that particularly

affect the low light performance, could also be invoked to explain the early morning behavior. However, the current-voltage characterization performed on both devices after lamination did not reveal shunt issues (Figure 16) so we consider this effect unlikely to occur. Note that this effect can also be seen in the evening hours, yet to a lower extent.

Overall observed trends: both samples feature initially a roughly similar behavior as the reference HJT device on sunny days, but a lag on cloudy days with full or partial recovery. Both samples then show a worsening of the recovery time after 1 year operation, that is superimposed to an increased overall degradation. The recovery time is observed to get longer as the device ages, which is also observed during indoor testing (see D3.3). Note that all selected days are in summer. Longer recoveries can be expected in winter (lower GPOA irradiance and temperatures), which is in-line with the “winter dip” revealed in Figure 2 and Figure 4. On a side note, we report on poor PR of the PST devices during early morning and late evening (sun behind neighboring mountains → diffuse skylight) already from day 1, the root causes of which is likely to be linked to a combination of low photogeneration in the bottom cell and the previously and regularly observed Light-Soaking Effect (LSE) in perovskite solar cells (see Section 4 for the state-of-the-art on that effect).

3.2.3. Energy loss: hard degradation vs. winter dip

In order to compare the individual effects on the energy yield of 1) the background long-term degradation trend and 2) the (mostly) reversible winter dip, we convoluted the PR reductions associated with both stages with the daily solar energy potential. As a rough approximation, we defined the PR losses associated with either effect as depicted in Figure 6. This exercise was performed for sample B1_HP2, which is the most stable device in this study.

Despite the apparent impressive dip shown in Figure 6, our calculation revealed yield losses of **only 2.7% caused by that “winter dip”, and 10.0% caused by the background degradation** (i.e. 4 times higher losses). We emphasize that these numbers should be considered as rough estimates, as some physical mechanisms are common to both stages (for instance we reported that the slow recovery effect, severely impacting on the winter PR, can also impact to some extent the energy production on summer days). **Nevertheless, it suggests that efforts should be dedicated first towards the improvement of the year-on-year stability (lower background degradation), which hopefully also goes hand-in-hand with an improvement in the winter PR behaviour.**

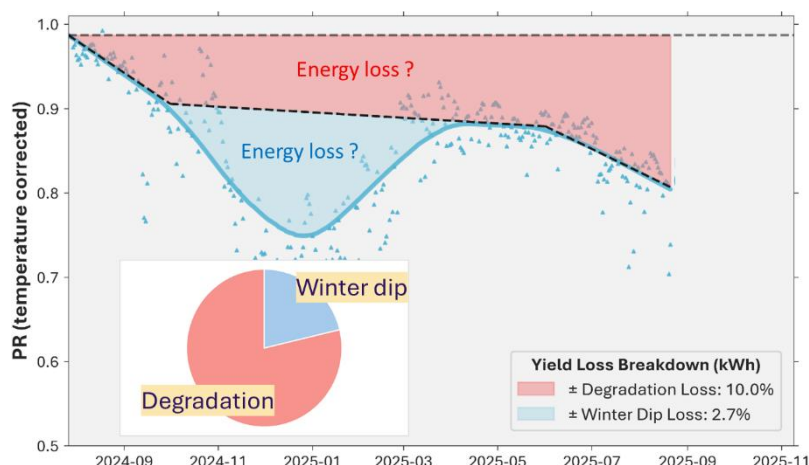


Figure 6 Yearly PR evolution and stages for B1_HT1 and corresponding Yield loss pareto.

3.3. Visual inspection of the two selected devices

Visual inspection was performed at different stages of the project. In the figure below, the photographs of the two samples of interest are shown at reception, installation (July 2024), after 3 months of monitoring and at the time of writing of this deliverable, i.e. after 14 months of monitoring.

For both samples, the photographs revealed a progressive contact discoloration highlighted in orange, that was already present after 3 months of monitoring. This is observed on the contact pads of the subcells, as well as on the interconnection strips (less clear). No clear signs of moisture ingress are present though (no colour gradients appeared for instance). B1_HP2 shows a quite distinct green coloration of the cell as well, but this coloration was already present from the start (and is most probably explained by the presence of an antireflective coating applied to the cell). The change of colour over time was not monitored - other than via mere photographs - so no conclusions can be drawn regarding the colour evolution.

In general, contact discoloration is associated with contact corrosion/deformation due to humidity ingress [3] and/or ion migration from the perovskite (iodine mainly). **Therefore an increased series resistance is suspected for both devices.**

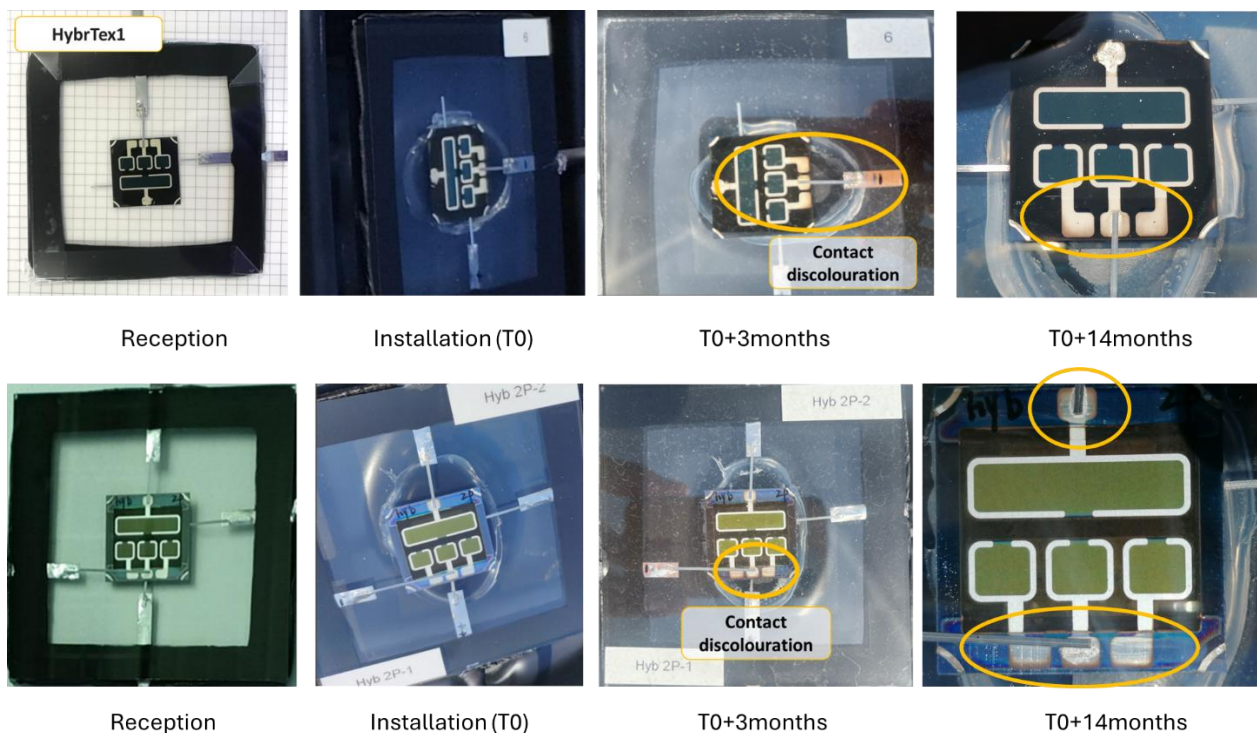


Figure 7 Photographs of the two devices analyzed in this report (bottom B1_HP2, top B1_HT1). The devices are still up and running at the time of writing of this report.

The back side of the samples did not show any evolution and are therefore not shown here.

4. Literature review and comparison with NEXUS results

4.1. Overview of outdoor stability results

As of today, there are only a handful of reports on outdoor stability [4-8]. This probably stems from the facts (among others) that the PST technology is relatively young, cell elaboration processes are of increased complexity compared to single junction perovskite cells, and encapsulation trials are still scarce. In Figure 8, we plot the outdoor monitoring duration as a function of the publication date for the different available studies. For those studies featuring over 1 year of monitoring (including ours), the year-on-year degradation rate is indicated. For the study by Remec et al. in 2024 [4], we estimated the degradation rate by extrapolating (rule-of-three) the data reported, as it covers a period shorter than a calendar year.

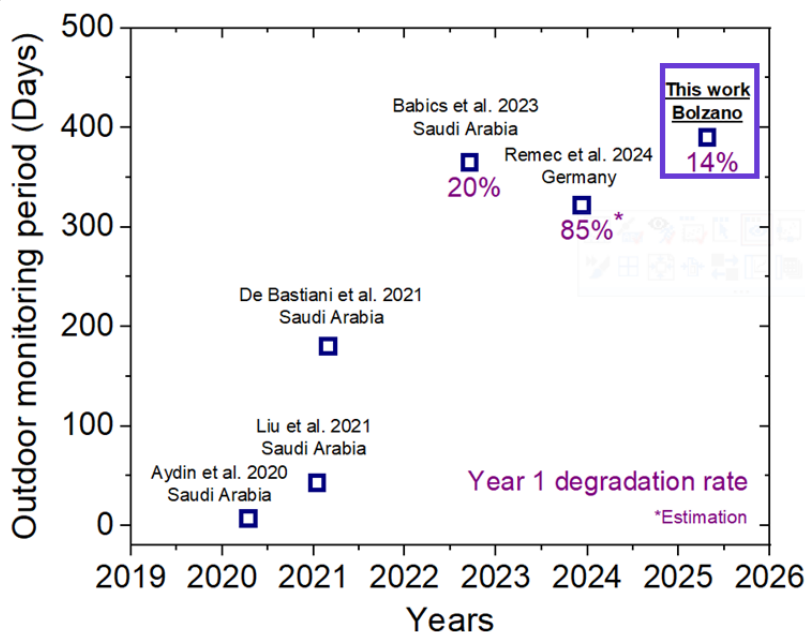


Figure 8 Overview of existing literature on outdoor monitoring of PST devices as per September 2025. The best result of the present study is shown in the purple rectangle.

As can be observed, and to the best of the authors' knowledge, **the most stable PST device in the present study features the most promising stability with a 14% year-on-year degradation**. This represents of course a **positive learning curve**, but most of all highlights the **necessity for outdoor stability improvements**. Indeed, the NEXUS partners concluded in Deliverable D4.1 *“Bankability report for a tandem PVSK/Si module based on outdoor measurements”* that, under such degradation rates and a realistic cost scenario, the PST technology does not achieve Levelized Cost of Electricity (LCOE) values comparable to those of mainstream high-efficiency silicon modules — even assuming an exceptional initial module efficiency of 34% (working hypothesis: 1 GWp fixed-tilt utility-scale PST plant located in Southern Europe over a 30-year lifetime).

4.2. Metastability in perovskite-containing devices

There is extensive literature reporting on the metastability of perovskite single junction solar cells during indoor lab testing (e.g. forward/reverse IV scans, MPP tracking, day/night cycling), since the first reports on early perovskite formulations [9] until recent observations on more advanced formulations

[10]. In general, the root cause of these effects is attributed to **ionic movement and defect passivation**. Under light or electrical bias, they induce redistribution of free carriers in the perovskite absorber, leading to transients in cell voltage (see for instance [11] and [12]).

Regarding outdoor testing of single junction perovskite cells, several very recent studies (2025) do report similar effects, typically referred to as “Light-Soaking Effect” (LSE) [4][10][13][14][15]. These authors report on transients at the beginning of the day, a representative and illustrative example of which is shown here below [4]. **The reported behavior features a slowly increasing voltage at the beginning of the day, which tends to stabilize in a second phase, in qualitative agreement with our observations (see below).**

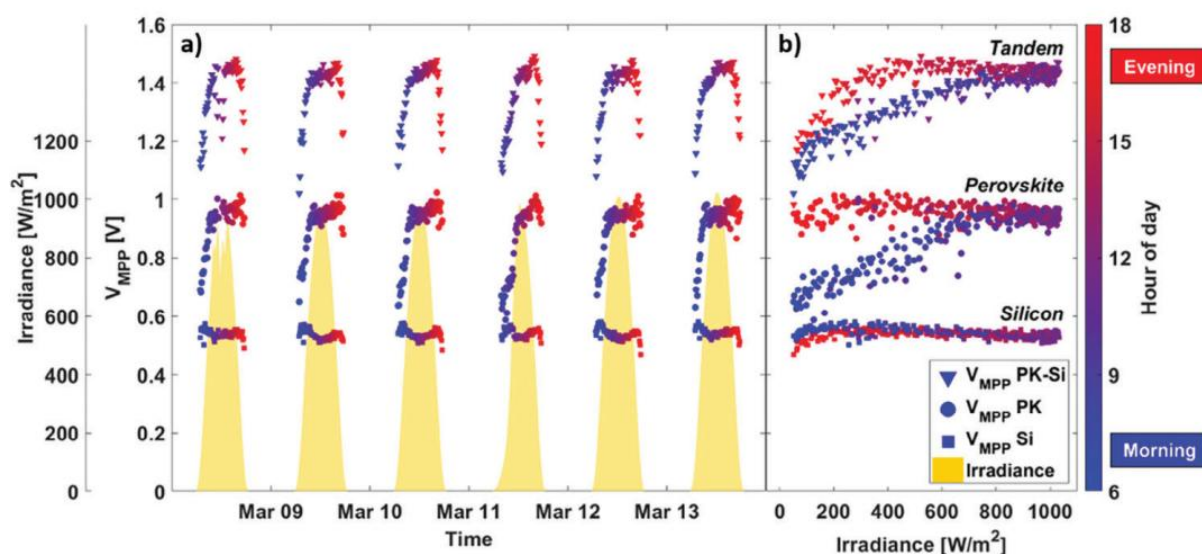


Figure 9 Typical materialization of the “Light-Soaking Effect” on single junction perovskite and PST devices during outdoor testing [4].

In the meantime, reports of similar effect on PST devices have started to multiply in the past years too [4-8]. Also in these studies, ionic movement of the perovskite top cell is generally reported to be the root cause of the observed phenomenon, which seemingly is logically inferred from the results on single junction solar cells.

From a parametrization of the LSE from their data, the authors in [4] quantified the LSE-related energy losses in and predicted that, for several locations in the USA, “...in winter, the [PST] device can lose a notable amount of the potentially generated energy due to LSE” and the reported calculated values lie between 1.9% and 3.1% (optimally oriented PK-Si tandem device, assumption that the LSE does not worsen nor improve over time). **In Section 3 we reported approximate losses of 2.7% due to the “winter dip”, which is in good quantitative agreement with their calculations.**

Interestingly, **perovskite-on-CIGSe tandem devices are also affected by the LSE effect**, with similar signatures as those encountered on PST devices [15].

Take-away messages: *From this brief overview of latest results, we can conclude that the lag/recovery effect observed on NEXUS devices in the above is not specific to the NEXUS top cells present in two studied devices, but rather seem to be a broader issue affecting devices obtained by different research groups, processes and compositions. Note that this effect is however not systematically affecting perovskite single junctions, for instance in [17] where the authors report on*

an “inverted” perovskite cell showing virtually no transient effects during day/night cycling tests (see Fig. 3 therein). This suggests that the issue could be effectively mitigated through appropriate process or compositional engineering of the perovskite top cell.

4.3. Influence of temperature on LSE effect

In [4], the authors attempted to isolate the influence of temperature only by means of simulation and measurements. They found a clear positive correlation between temperature and kinetics of the LSE effect (see Figure below) and could describe the kinetics of the LSE using an Arrhenius function.

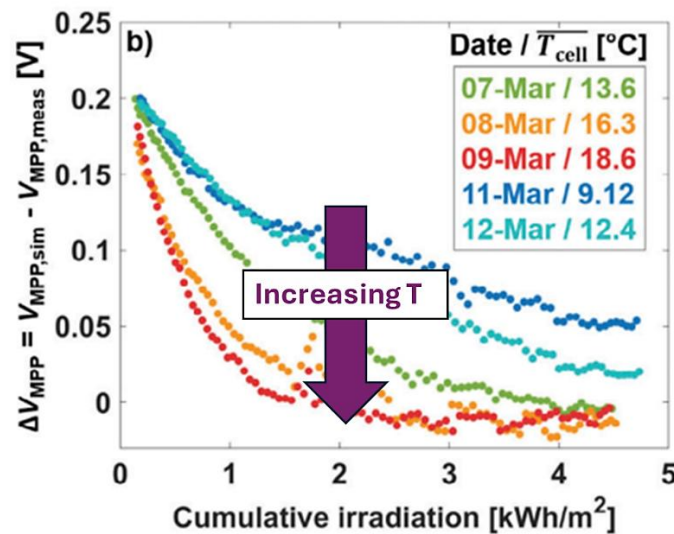


Figure 10 Light-Soaking Effect kinetics for several consecutive days in March 2022, plotted as a function of the daily cumulative irradiation. The days featured “very similar irradiance conditions”. $V_{mpp,sim}$ is the expected V_{mpp} without LSE, as derived per simulations. Adapted from [4].

We attempted to extract the specific effect of temperature on the recovery effect kinetics by checking how the PR is affected by cell temperature at a given GPOA irradiance (B1_HT1). However, due to fast device aging in our case, we had to restrict the useful data to short time ranges at the beginning of the monitoring campaign, which yielded small datasets. We nevertheless show the results in Figure 11 for the sake of completeness, which show the daily PR as a function of daily GPOA irradiance and device (max or mean) temperature. As can be seen, Figure 11 does not reveal a clear PR trend as a function of temperature if we fix the GPOA irradiance (more data point are needed). For that reason, and also recalling that the spectrum effect can be non-negligible, we refrain from concluding.

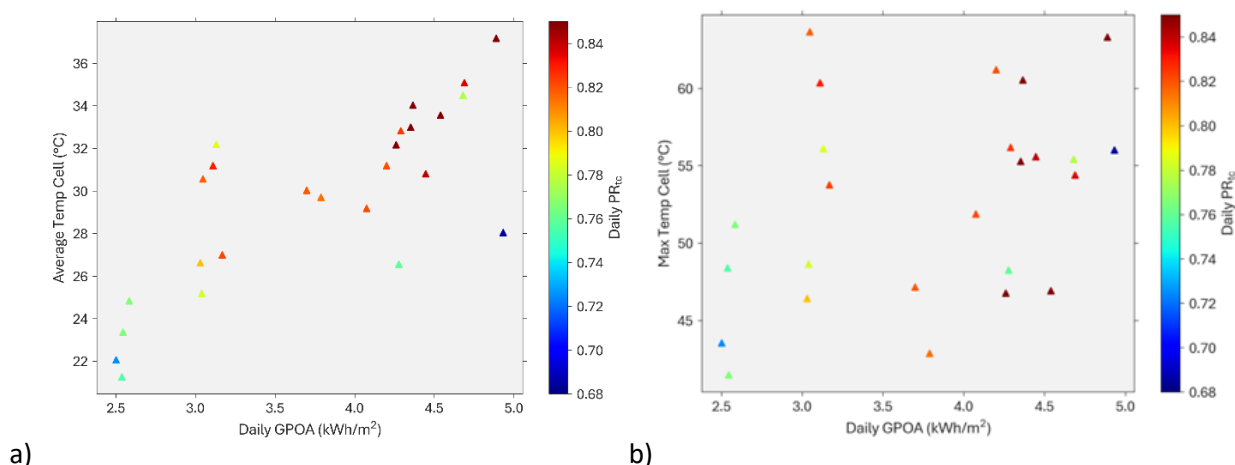


Figure 11 Daily PR as a function of daily GPOA irradiance and a) average device temperature and b) maximum device temperature (this study)

This being said, the results presented in Figure 4, where we analysed the daily PR data over >1 year as a function daily GPOA irradiance, evidenced that, for a given daily GPOA irradiance, the PR was significantly lower in winter (data points shown in purple in Figure 4). Even if here again spectral effects could play a central role, it is in qualitative agreement with a slower recovery / LSE on days with low temperature¹, in line with findings from Remec et al. [4].

5. Discussion

In this section, we summarize the key observations from the previous sections and propose phenomenological explanations. When the root cause(s) cannot be identified, we nevertheless aim to narrow down the range of plausible explanations.

In Section 3, two striking features were identified on the PR evolution through 1 year of operation: a **background performance degradation**, superimposed by a (at least partly) reversible loss around winter time referred to as the **“winter dip”**.

Background degradation:

The background degradation is characterized by a **progressive reduction in PR mostly during high irradiance days** (Figure 4), and to a lesser extent during medium irradiance days (and only marginally during low irradiance days). It materializes as two effects: 1) a **lower saturated PR value during high irradiance days** (Figure 5), as well as 2) a **morning recovery that seems to get slower with aging time** (Figure 5) for days with similar temperature profiles and daily irradiances. Regarding effect 1), a possible explanation (non-necessarily exhaustive) would be a **major increase in the device series resistance**, that is known to affect the efficiency more strongly at high irradiances (higher current = higher ohmic losses), consistent with our observation. This hypothesis is further supported by the

¹ In absolute, ion motion (believed to be the root cause of solar perovskite metastability) is typically limited by diffusion and it would therefore be highly unlikely that the LSE kinetics would not show a positive correlation with temperature.

visual inspection of the devices, which reveals a progressive **darkening of the contacts**, interpreted as **contact corrosion** induced by humidity ingress (Figure 7). The possible origin of effect 2) is discussed hereafter.

Interestingly, we found that the PR in the lowest GPOA irradiance regime was mostly invariable throughout the monitoring period (Figure 4). If the shunt resistance were to drop during outdoor exposure, such invariance would not be observed. Instead, a progressively larger fraction of the – small - photogenerated current would be lost through the shunt resistances, which would particularly affect the efficiency and thus the PR on such low irradiance days. As this is not observed in practice, we conclude that if there is a worsening of the shunt resistances during outdoor exposure, then this worsening is minor. In other words, **our results do not suggest a large (if any) degradation of the shunt resistances of the devices.**

“Winter dip”:

Some possible root causes that can explain a lower PR in cold dark days are the following, possibly operating in parallel [4]:

- **low (absolute) shunt resistance.** Initial IV characterization did not reveal particularly low device shunt resistance, in any case not for B1_HP2 (see Figure 16). This explanation is therefore **unlikely**.
- **metastability effects.** Such metastability has been evidenced in Figure 5 for summer days (Light-Soaking Effect, LSE) and, building on literature, it is **very likely that is strongly impacts on the winter PR**. The low flyer winter data in Figure 4 further supports that view. Note that such metastability is rather typical of other thin film technologies such as CdTe or CIGS, which typically require exposure to light in order to reach the full potential of the device [18].
- **Current mismatch effects** due to strong deviations from the AMG1.5 spectrum. A detailed spectral analysis was outside of the scope of the present study but is highly recommended for future studies.
- At low temperatures, other effects could be due to **freezing of trapped ions** in configurations prone to increase carrier recombination, or **increased interface barriers (series resistances)**.

Extending the discussion on the perovskite metastability (LSE): we evidenced that low irradiance days are associated with a slow increase of PR in the morning hours (Figure 5), and that the PR may even fail to reach full recovery in the course of such a day. We also observed that after a particularly low irradiance day, the PR may need several medium/high irradiance days to fully recover (Figure 3), suggesting that the **history of the sample** - i.e. how warm/bright the previous days were - **may be necessary to predict the PR behaviour on day N**. This effect would be related to **ions of the perovskite absorber**, that migrate through the device following the local band bending, which is different whether the device is illuminated or not. In the first moments of the day, the ions would **move from their night position to their day position** at a limited speed (diffusion-limited) and with a different driving force depending on the band-bending, itself depending on carrier photogeneration and ultimately on irradiance. This theoretical framework is able to qualitatively explain the PR morning recovery and its apparent dependence on GPOA irradiance and/or temperature that we report in Figure 4 and Figure 5.

6. Concluding remarks and outlook

In this work, we analysed in detail the outdoor stability of the two front-runner NEXUS devices installed at Eurac Research, Bolzano, Italy, with over a year of testing. The best sample was found to exhibit a 14% year-on-year degradation rate. Although such value demonstrates the positive learning curve of the PST community, it also calls for action to improve device stability and ultimately the business case for PST modules.

Through the study of the data at seasonal, daily, and hourly levels, we study the key features of the background degradation and the (mostly reversible) metastability effect, both phenomena occurring simultaneously. Through a comparison with existing (scarce) literature, we evidenced that the metastable effects are common to most devices reported in the recent literature, but that it can also be mitigated/suppressed by engineering the top cell composition/architecture. If not properly tackled, such metastability effects could restrict the use of PST in regions with favourable climates, i.e. warm and sunny. It is therefore of high importance that both the background degradation and the metastability effect be monitored and communicated to cell and module engineers for “field-inspired” continuous device improvement. Additionally, decoupling irradiance and temperature effects should also be attempted in future studies to specify the mechanisms at play. So far, the devices of interest are still being monitored to extend the monitoring dataset. Forensics will be performed once the devices will be decommissioned, in order to put the above-listed working hypothesis to the test.

References

- [1] J. Veirman et al., “Outdoor Performance and Reliability of Perovskite (Pk)-Silicon (Si) Tandems”, presented at the 42nd EU-PVSEC, Bilbao, Spain, Sept. 2025
- [2] H. Quest, et al. "Decoupling performance gains of Silicon Hetero-Junction bifacial modules, WCPEC-8 2022, 26 – 30 September 2022, Milano, Italy.
- [3] IEA PVPS, “Photovoltaic Failure Fact Sheets (PVFS) 2025”. Accessed online on October the 23rd 2025. <https://iea-pvps.org/wp-content/uploads/2025/02/IEA-PVPS-T13-30-2025-PVFS-ANNEX-Degradation-and-Failure.pdf>
- [4] M. Remec et al., “From Sunrise to Sunset: Unraveling Metastability in Perovskite Solar Cells by Coupled Outdoor Testing and Energy Yield Modelling.” *Advanced Energy Materials*, 2024, 14, 2304452. DOI: 10.1002/aenm.202304452
- [5] M. Babics et al., “One-year outdoor operation of monolithic perovskite/silicon tandem solar cells”, *Cell Reports Physical Science*, Volume 4, Issue 2, 15 February 2023, 101280. <https://doi.org/10.1016/j.xcrp.2023.101280>
- [6] M. De Bastiani et al., “Toward Stable Monolithic Perovskite/Silicon Tandem Photovoltaics: A Six-Month Outdoor Performance Study in a Hot and Humid Climate”, *ACS Energy Lett.* 2021, 6, 2944–2951. <https://doi.org/10.1021/acsenerylett.1c01018>
- [7] J. Liu et al., « 28.2%-efficient, outdoor-stable perovskite/silicon tandem solar cell », *Joule*, Volume 5, Issue 12, 15 December 2021, Pages 3169-3186. <https://doi.org/10.1016/j.joule.2021.11.003>
- [8] E. Aydin et al., « Interplay between temperature and bandgap”, *Nature Energy*, volume 5, pages851–859 (2020). DOI: <https://doi.org/10.1038/s41560-020-00687-4>
- [9] E. T. Hoke et al., “Reversible photo-induced trap formation in mixed-halide hybrid perovskites for photovoltaics.” *Chemical Science*, 2015, 6, 613–617. DOI: 10.1039/c4sc03141e
- [10] M. Remec et al., “Seasonality in Perovskite Solar Cells: Insights from 4 Years of Outdoor Data” *Advanced Energy Materials*, 2025, 15(35), 2501906. DOI: 10.1002/aenm.202501906
- [11] J. Herterich et al., “Ion Movement Explains Huge VOC Increase despite Almost Unchanged Internal Quasi-Fermi-Level Splitting in Planar Perovskite Solar Cells”, *Energy Technol.* 2021, 9, 2001104. DOI: 10.1002/ente.202001104
- [12] Bian et al., “Unravelling of the reversible light soaking mechanisms in intrinsic halide perovskite film”, *J. of Power Sources* 653 (2025) 237704. <https://doi.org/10.1016/j.jpowsour.2025.237704>
- [13] M. G. De Ceglie et al., “Intraday Outdoor Efficiency Changes in Metal-Halide Perovskite Photovoltaic Modules.” *IEEE Journal of Photovoltaics*, 2025, 15, Article 3575469. DOI: 10.1109/JPHOTOV.2025.3575469
- [14] Gupta et al., “Seasonal Effects on Outdoor Stability of Perovskite Solar Cells.” *Advanced Energy Materials*, 2025. DOI: 10.1002/aenm.202570041
- [15] G. Bovesecchi et al., “Outdoor Performance Monitoring Method for Degradation Studies of Perovskite Modules.” *Progress in Photovoltaics: Research and Applications*, 2025, 33(3), 445-461. DOI: 10.1002/pip.3860.
- [16] G. Farias-Basulto et al., “Perovskite-CIGSe Tandem Solar Cell: Over One Year of Outdoor Monitoring.” *Advanced Energy & Sustainability Research*, 2025, Article 2500162. DOI: 10.1002/aesr.202500162.
- [17] L. Jiang, “Fatigue stability of CH₃NH₃PbI₃ based perovskite solar cells in day/night cycling”, *Nano Energy* 58 (2019) 687–694 . <https://doi.org/10.1016/j.nanoen.2019.02.005>
- [18] M. Gostein & L. Dunn, “Light Soaking Effects on Photovoltaic Modules: Overview and Literature Review.” *Proceedings of the 37th IEEE Photovoltaic Specialists Conference (PVSC)*, Seattle, USA, 2011, pp. 003138–003143. DOI: 10.1109/PVSC.2011.6186310

Annex 1: Promising devices (<12 months monitoring)

Devices were installed at the four project partners (FHNW, Eurac Research, GUNAM, UVEG) in the course of the project. Some devices have been installed less than 12 months ago, so *per se* cannot be the focus of this deliverable. Nevertheless, they show promising monitoring data at the end of the project and we hence briefly present the results here below.

Devices installed at GUNAM, Ankara, Türkiye:

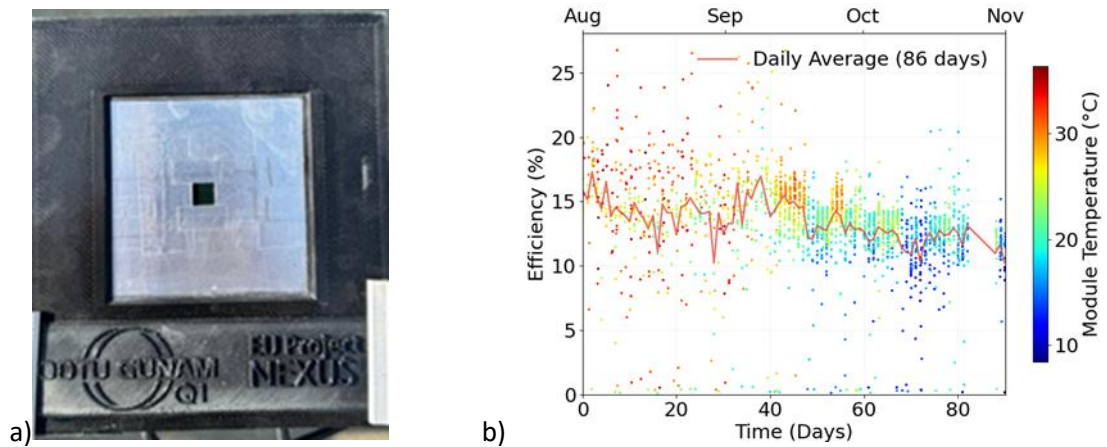


Figure 12: a) Photograph of the O1 device from KIT and installed at GUNAM, Ankara, Türkiye. b) Efficiency tracking as a function of time (~3 months). Each data point was derived from a current-voltage measurement taken every 10 minutes. The sample is kept at maximum power point between two consecutive measurements. Monitoring start: August 2025.

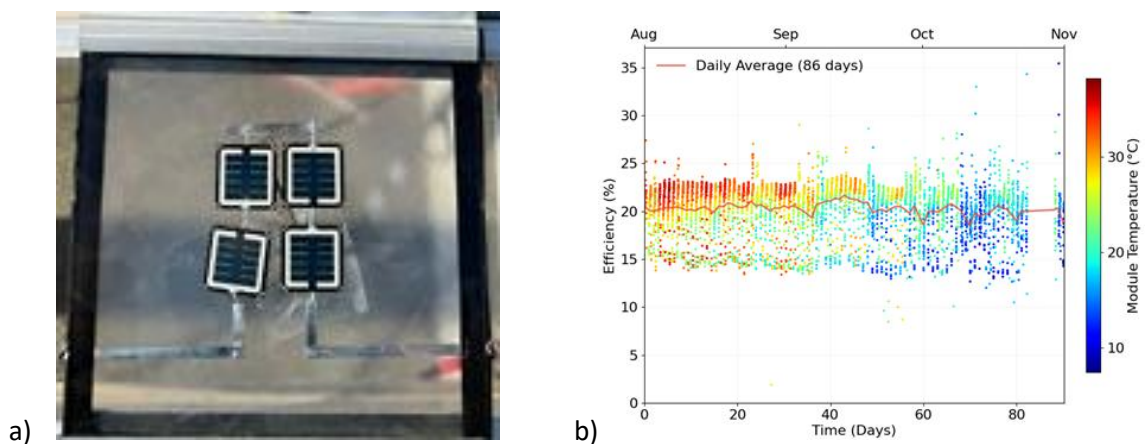


Figure 13: a) Photograph of the sequentially evaporated (from UOXF) 4-cell tandem module from CEA and installed at GUNAM, Ankara, Türkiye. These cells incorporate the nanotextured Si with a thin ITO interlayer and the rear AZO electrode. b) Efficiency tracking as a function of time (~3 months). Each data point was derived from a current-voltage measurement taken every 10 minutes. The sample is kept at maximum power point between two consecutive measurements. Monitoring start: August 2025.

Both devices, about 18-19% STC efficiency, are showing promising stabilities after some

months of monitoring. The interested reader is referred to D4.6 deliverable Report on the outdoor performance of PVSK/Si minimodules in Ankara climate, where the results are presented in more detail, along with other devices that have been tested at this location.

Devices installed at UVEG, Valencia, Spain:

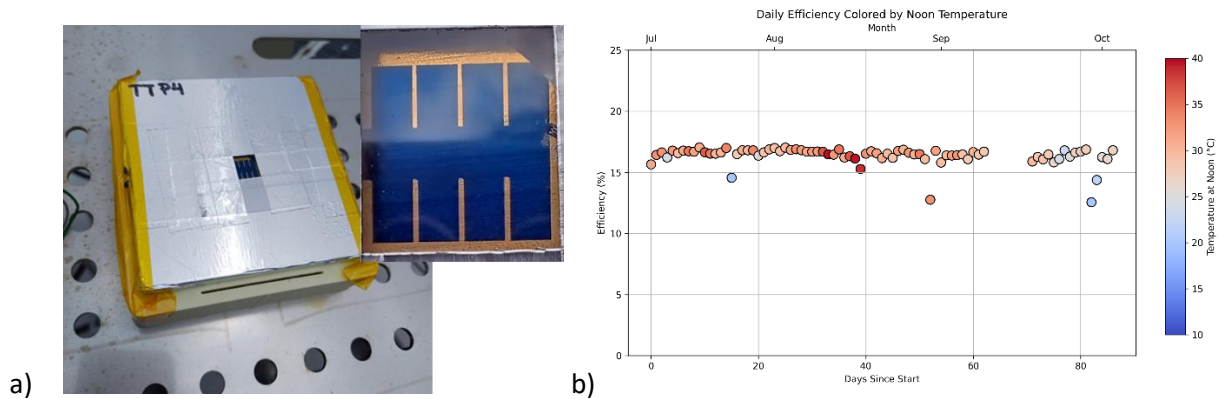


Figure 14: a) Photograph of the device from KIT (lamination at CEA) and installed at UVEG, Valencia, Spain. b) Efficiency tracking as a function of time (3 months). The sample is kept at maximum power point between two consecutive measurements. Monitoring start: February 2025. Monitoring end: July 2025.

This sample (TTP4) retains about 17% efficiency after about 3 months of monitoring, showing no sign of instability so far.

Other devices installed at Eurac Research, Bolzano, Italy:

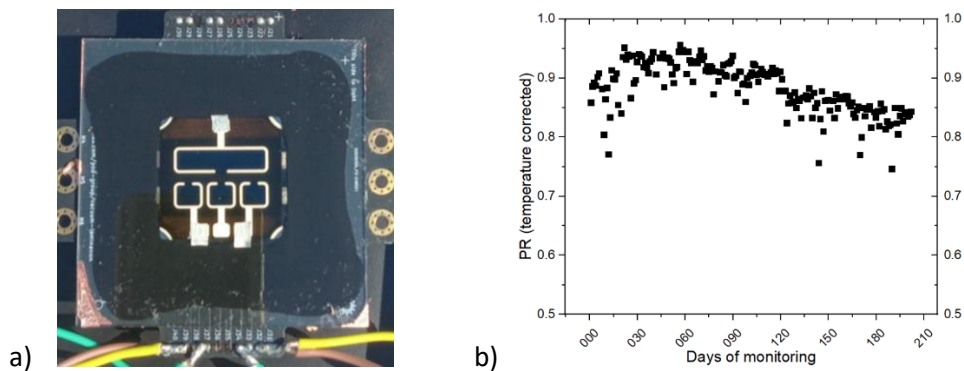


Figure 15: a) Photograph of the device from Oxford Uni (lamination at CEA) and installed at Eurac Research, Bolzano, Italy. b) Temperature-corrected performance ratio as a function of time (roughly 7 months). The sample is kept at maximum power point throughout the monitoring campaign. Monitoring start: February 2025.

Although all these samples have been monitored for short periods of time, thereby disqualifying them for the analysis in this report, they hold promise for the long term stability of the devices made in the NEXUS project.

Annex 2: Initial IV curves of the two studied PST devices

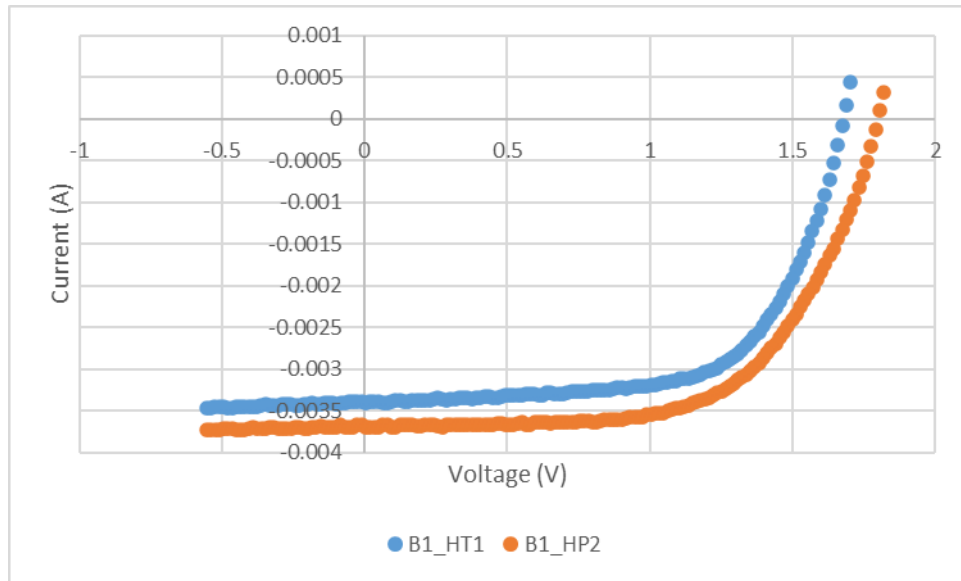


Figure 16: Initial current-voltage curves of the two studied PST devices, measured after lamination.